

DEVELOPMENT OF AN ANALYTICAL SOLUTION FOR COMPRESSIBLE TWO-PHASE STEAM FLOW

M. Zayernouri M. J. Kermani¹
Department of Mechanical Engineering
Amirkabir University of Technology (Tehran Polytechnic),
Tehran, Iran, 15875-4413
¹Corresponding Author
E-mail: mkermani@aut.ac.ir

Received November 2005, Accepted March 2006
No. 05-CSME-63, E.I.C. Accession 2915

ABSTRACT

An analytical solution for the isentropic expansion of subsonic-supersonic two-phase steam flow is provided in this paper. The results are supported by our earlier numerical computations, and available experimental values of others (1973). The two-phase mixture is assumed to undergo an isentropic expansion. However the entropy of the vapor portion of the two-phase mixture increases as the released latent heat of the condensate, reversibly moves toward the vapor, and enhances its entropy, as well as the so called "local stagnation" temperature of the vapor. The mass flow rate of the vapor portion of the two-phase mixture is obtained based on the "local stagnation" conditions, and then corrected to give the mixture mass flow rate. Most of the attempts have been made to develop the solution in a manner similar to those of the ideal gases.

DEVELOPPEMENT D'UNE SOLUTION ANALYTIQUE POUR LE FLUX DIPHASIQUE DE VAPEUR COMPRESSIBLE

RESUME

Une solution analytique pour la détente à l'entropie constante du flux diphasique de vapeur subsonique-supersonique est fournie dans cette communication. Les résultats sont soutenus par notre calcul numérique précédent et aussi par les valeurs expérimentales disponibles (1973). Le mélange diphasique est supposé pour subir une détente à l'entropie constante. Cependant l'entropie de la portion de vapeur dans la mélange diphasique augmente quand la chaleur latente relâchée du condensat réversiblement se déplace vers la vapeur, et améliore son entropie. de même que appelé la température de "stagnation locale" de la vapeur. Le débit massique de la portion de vapeur du mélange diphasique est obtenu basant sur les conditions de "la stagnation locale", ensuite ce débit massique a été corrigé alors pour donner le débit massique de mélange. La plupart de tentative a été fait, à fin de développer la solution dans une manière similaire à ceux des gaz portraites.

1 INTRODUCTION

The fundamental equation for isentropic expansion of an ideal gas can be written as:

$$pv^\gamma = \text{Constant} \quad (1)$$

where p and v are the pressure and specific volume of the gas, respectively, and γ is the specific heat ratio, which is taken to be constant along the process with values of ≈ 1.4 for air or 1.32 for dry steam. In two-phase flows the usage of similar formulae has also been reported at the expense of loosing some accuracy, [1], in which an averaged value for γ is used along an isentropic process. This approach has limited applications; especially when accurate and detailed information of the moisture content is needed. Correct prediction of moisture levels in multi-phase wet flow applications is a vital issue.

For two-phase mixtures, the relationship between the pressure and specific volume does not obey Eqn. 1, and an alternate approach is needed. In such processes, the stagnation properties of the vapor portion of the two-phase mixture are variant, because of the flow of latent heat towards the vapor. Therefore, it is necessary to extract a new formula for the local stagnation state in order to obtain the characteristics of the flow field. To do so, the experimental studies [2, 3, 4] have been done to find the total pressure of compressible two-phase (wet) flows. In addition, a unified theory to interpret the total pressure and temperature in the two phase (wet) flow has been developed introducing a variable but equivalent equilibrium isentropic exponent γ [5]. These approaches require additional attempts to obtain the variable exponent γ . Moreover, depending on how deep the flow expands under the saturation dome, a more comprehensive knowledge of γ will be required. The use of variable γ usually adds excessive complexities to the solution, which is generally preferred to avoid when analytical solutions are sought. In the present study most of the attempts have been made to give a series of formulae, in a form similar to those for the perfect gases, .i.e. with constant specific heat values and γ . The appearance of the developed formulae are very similar to those reported in fluid mechanics or thermodynamics texts, e.g. [6]. This makes the usage of the present formula very user friendly.

The present work follows the numerical computation of compressible two-phase steam flow through converging-diverging nozzles [7, 9], which was supported by experiments of Moore et al. [8]. The main contribution of the present paper is to give an analytical solution to predict the isentropic expansion of compressible two-phase steam flow in a closed form.

The paper briefly explains our earlier numerical approach [7], which is based on Roe's Flux Difference Splitting scheme. Then a complete procedure of the development of the analytical approach is provided in details. This is followed by a step by step handy and practical flow-chart summarizing all the detail. In the development process, a local vapor-side stagnation condition has also been defined, which reflects the stagnation condition of the vapor portion of the mixture, and differs from that of the inflow. Finally the analytical results are compared with numerical computations and experimental data. The comparison shows excellent agreement.

2 NUMERICAL SOLUTION

The numerical approach is explained in an earlier publication [7], which is briefly repeated here for the completeness purposes. The convective and pressure terms of the governing equations of fluid motion are discretized using Roe's FDS density-based scheme. For dry regions, the pressure (p), temperature (T), and velocity (u) are extrapolated to cell faces by the MUSCL approach using a third-order upwind-biased scheme, [10] while in wet regions T , u and the quality (χ) are used for extrapolation purposes. Pressure in two-phase regions is, therefore, equated to the saturated pressure at the local temperature according to equilibrium thermodynamic model. The Roe-averaged value at the cell faces is obtained based on mixture

(liquid + vapor) properties at the sides of the cell faces. The van Albada flux limiter is used to prevent spurious numerical oscillations.

The governing equations of fluid motion for quasi one-dimensional, unsteady, compressible flow in full conservative form and with no body forces can be written as [11]:

$$\frac{\partial}{\partial t}(SQ) + \frac{\partial F}{\partial x} - H_s = 0, \quad (2)$$

where x and t are the space and time coordinates, S is the cross sectional area of the duct, Q , F , and H_s respectively represent, the conservative vector, the flux vector and the source term, given by:

$$Q = \begin{bmatrix} \rho \\ \rho u \\ \rho e_t \end{bmatrix}, \quad F = S \begin{bmatrix} \rho u \\ \rho u^2 + p \\ \rho u H \end{bmatrix}, \quad H_s = \frac{dS}{dx} \begin{bmatrix} 0 \\ p \\ 0 \end{bmatrix}.$$

Here, ρ is the two-phase mixture density, u is the velocity, e_t is the total mixture energy, p is the pressure, and H is the total enthalpy of the two-phase mixture. For the present study of low pressure steam flow at pressures below one atmosphere, the ideal gas equation of state: $p = \rho_g RT$ is of sufficient accuracy, in which ρ_g is the vapor-side density and R is the gas constant ($= 461.3990$ J/kg.K for vapor) and $h_{fg} = e_{fg} + RT$, where e_{fg} is the change in internal energy from the saturated liquid state to that of the saturated vapor (see Appendix A for e_{fg} as a function of temperature). The governing equations, Eqn. 2, are subjected to the following boundary conditions: The inflow is subsonic and assumed to be dry, for which the stagnation pressure and temperature are specified. At the exit plane for which supersonic conditions prevail, all flow properties are extrapolated from the interior domain.

The numerical flux for Roe scheme is calculated from the L and R states on both sides of a cell face. For dry flow conditions, this has been well explained in several text books. However, for two-phase flows, it should be noted that the gas properties are replaced by those of the two-phase mixture. For example, density and total enthalpy for the East face of a control volume is obtained using:

$$\hat{\rho}_E = \sqrt{\rho_E^L \rho_E^R} \quad \hat{H}_E = \frac{\sqrt{\rho_E^L} H_E^L + \sqrt{\rho_E^R} H_E^R}{\sqrt{\rho_E^L} + \sqrt{\rho_E^R}} \quad (3)$$

where all the properties in wet regions correspond to the mixture values. For example, the values at the Left (L) side of the East (E) face are:

$$\underbrace{\rho_E^L}_{\text{two-phase mixture density}} = (\rho_g)_E^L / (\chi)_E^L \quad (4)$$

and

$$\underbrace{H_E^L}_{\text{two-phase mixture enthalpy}} = \underbrace{(h_f)_E^L + (\chi)_E^L (h_{fg})_E^L}_{\text{two-phase mixture enthalpy}} + \frac{1}{2} [(u)_E^L]^2. \quad (5)$$

As the solution marches in time, the conservative vector Q is updated at each time level. Q provides values for two-phase mixture density and total internal energy. Knowing the value of velocity at the same time level, a static value of the internal energy can be obtained. The thermodynamic state point can then be fixed based on current values of two-phase mixture density and internal energy. The moisture content (the quality), if present can then be determined. The numerical solution were compared by experiments of [8]. Complete information is provided in [7].

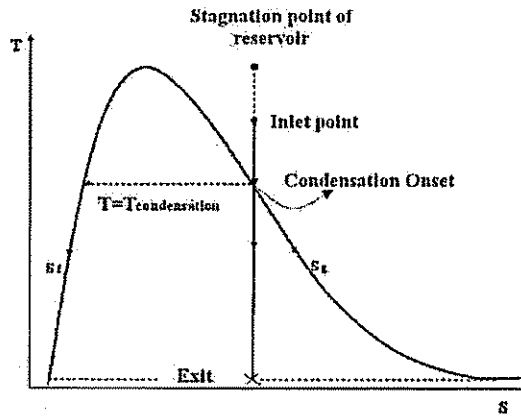


Figure 1: T-S diagram for an isentropic expansion of steam flow through a converging-diverging nozzle. As the two-phase flow expands along an isentropic line, its projection follows the saturated vapor (g) and saturated liquid (f) curves.

3 DEVELOPMENT OF ANALYTICAL SOLUTION

An analytical solution for the isentropic expansion of condensing steam flow is given in this section. The model is based on an equilibrium thermodynamic model, which assumes that the second phase is generated as soon as the saturation line is crossed. This is performed in a step by step procedure, in which most of the attempts have been made to develop the formulae in a form similar to those of the perfect gases. A summary of the steps to obtain the analytical solution, and a flow chart describing the solution procedures are given in Sec. 4.

In this section a relationship is developed between the temperature and Mach number for an isentropically expanding two-phase mixture. For the present study, stagnation conditions of the dry steam at the nozzle inlet are provided. These are conditions at an imaginary reservoir upstream of the nozzle inlet with the pressure and temperature of $P_{0,res.}$ and $T_{0,res.}$, respectively, labelled as "reservoir" in Fig. 1. Dry steam from this imaginary reservoir isentropically accelerates to the inlet face of the nozzle, where its pressure and temperature are P_i and T_i , respectively. Further expansion of the flow through the nozzle, makes the flow cross the saturation line at a point so called "condensation onsets", and noted by "c.o." in this study (see Fig. 1), where condensation onsets according to the present equilibrium thermodynamic model. The entropy in the reservoir state is obtained using:

$$S_{0,res.} = C_p \ln(T_{0,res.}) - R \ln(P_{0,res.}). \quad (6)$$

In Eqn. 6, C_p and R are the iso-baric specific heat and the gas constant of the vapor, respectively. For an isentropic expansion of the flow from reservoir to "c.o.", one can write:

$$S_{c.o.} = S_{0,res.} \quad (7)$$

Knowing the value of $S_{c.o.}$ and equating this to the entropy of the gas phase, $S_g(T)$, the temperature at "c.o.", $T_{c.o.}$, can be obtained by:

$$S_g(T_{c.o.}) = S_{0,res.} \quad (8)$$

The corresponding pressure ($= P_{c.o.}$) is the saturation pressure at $T_{c.o.}$. The point "c.o." plays a key role in the present study, as it is the boundary between the dry and wet regions. For an adiabatic expansion of an

ideal gas, the following equation of classical gas dynamics is applied:

$$\frac{T_0}{T} = 1 + \frac{\gamma - 1}{2} M^2. \quad (9)$$

From "res." to "c.o.", the vapor is dry and can be assumed to be an ideal gas. Therefore,

$$\frac{T_{0,res.}}{T_{c.o.}} = 1 + \frac{\gamma - 1}{2} M_{c.o.}^2, \quad (10)$$

where $M_{c.o.}$ is the Mach number at "c.o.", and $\gamma = 1.32$ is the specific heat ratio of the dry steam. In Eqn. 10, with the values of $T_{0,res.}$ and $T_{c.o.}$ being known, $M_{c.o.}$ is, therefore, determined. Depending on the value of $M_{c.o.}$ three different scenarios could occur. (A): $M_{c.o.} > 1$, (B): $M_{c.o.} = 1$, and (C): $M_{c.o.} < 1$. It is noted that for all the three cases, the flow leaving the nozzle is supersonic. Hence, the nozzle throat needs to remain choked for all the cases.

In Case (A), condensation occurs downstream of the throat, therefore, $M_{c.o.} > 1$, as shown in Fig 2-A. In this case the choked mass flow through the dry-throat nozzle is obtained according to the classical gas dynamic equation, see [6] for example:

$$\dot{m}_{max (dry-throat)} = \frac{P_{0,res.} A^*}{\sqrt{R T_{0,res.}}} \sqrt{\gamma \left(\frac{2}{\gamma + 1}\right)^{\gamma + 1/\gamma - 1}}, \quad (11)$$

where A^* is the cross sectional area at the sonic throat. In nozzle (B), condensation occurs right at the throat, $M_{c.o.} = 1$ (see Fig 2-B). Since this point is on the saturation vapor line, the throat is still dry, and the mass flow rate can be obtained from Eqn. 11. In nozzle (C), condensation occurs upstream of the throat; where the flow is subsonic, i.e. ($M_{c.o.} < 1$). Therefore, the throat is wet. In this case, the stagnation conditions at the nozzle throat will not be the same as those at the reservoir. Therefore, Eqn. 11 will not represent the mass flow through the wet-throat nozzle. The physical features for the nozzle of Fig. 2-(C) are highlighted below:

1. The throat is wet.
2. For the adiabatic nozzle, the latent heat of the condensing portion of the steam (from "c.o." to the nozzle throat) should be somehow transferred from the condensate to the vapor side.
3. As a result of the released transferring heat towards the gas (vapor) side, the stagnation conditions of the gas phase are changed, i.e. $P_{0,local} \neq P_{0,res.}$, and $T_{0,local} \neq T_{0,res.}$.
4. Also, the entropy of the gas portion of the mixture will locally and continuously rise. On the other hand the entropy of the liquid portion will drop. The net effect is that the mixture entropy remains unchanged, as the whole process moves along an isentropic line.
5. As a result of continual condensation along the nozzle, gas phase mass flow rate continuously decreases, therefore, Eqn. 11 cannot be used to calculate the total mass flow rate.

Sections 3.1 to 3.5 discuss how the present analytical solution for a condensing flow has been developed.

3.1 Temperature vs. Mach Number

In this section a relationship between the temperature and Mach number for a two-phase steam flow is developed. Consider Fig. 2-C again, which is enlarged and shown in Fig. 3. The figure shows a control volume surrounding the nozzle inlet, where the flow enters as dry, and exits the control volume as wet

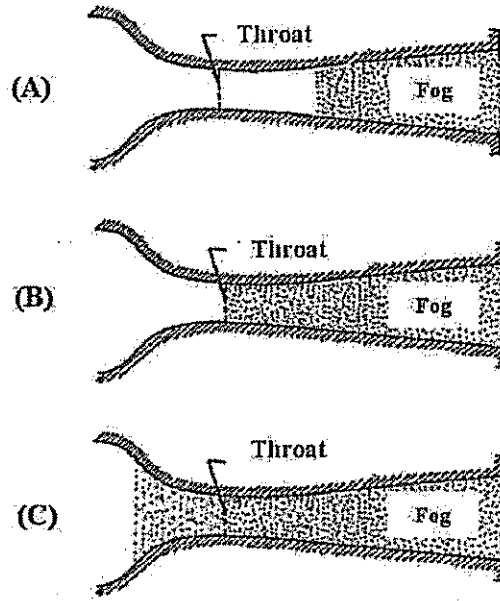


Figure 2: In nozzle *A* condensation occurs downstream of the throat (i.e. the throat is dry and $M_{c.o.} > 1$), in nozzle *B* condensation onsets right at the throat (i.e. $M_{c.o.} = 1$), and in nozzle *C* condensation occurs upstream of the throat (i.e. the throat is wet and $M_{c.o.} < 1$).

(two-phase). The exit location has been chosen arbitrarily, and in this section it is aimed to develop a relation between the mixture temperature and Mach number at this exit section. Applying the first law of thermodynamics around the control volume (in steady condition), we can write:

$$\dot{Q}_{c.v.} - \dot{W}_{c.v.} = \sum \dot{m}_e (h_e + \frac{V_e^2}{2} + gZ_e) - \sum \dot{m}_i (h_i + \frac{V_i^2}{2} + gZ_i). \quad (12)$$

With adiabatic wall-bounded boundaries, and assuming no work is crossing the boundary, also ignoring the body forces, Eqn.12 yields to:

$$\dot{m} h_{0,res.} = \dot{m}_g (h_g + \frac{V_g^2}{2}) + \dot{m}_f (h_f + \frac{V_f^2}{2}), \quad (13)$$

where $h_{0,res.}$ is the stagnation enthalpy of the reservoir, \dot{m} is the mass flow entering the nozzle, which is equal to the sum of \dot{m}_g and \dot{m}_f for steady-state conditions, and the subscripts *f* and *g* refer to fluid and gas, respectively (see Fig. 3). We assume that the vapor portion of the two-phase mixture is a perfect gas, and ignore the slip velocity between the phases, $V_f = V_g = V$, and divide both sides of Eqn. 13 by \dot{m} and use $h = C_p T$ for the gas-side, then:

$$C_p T_{0,res.} = \chi (C_p T + \frac{V^2}{2}) + (1 - \chi) (h_f + \frac{V_f^2}{2}) \quad (14)$$

where χ is the quality.

It is noted that the values of T , χ , and V correspond to an arbitrary exit plane of the control volume shown in Fig. 3. Taking $h_{fg} = h_g - h_f$, Eqn. 14 gives:

$$\frac{T_{0,res.}}{T} = 1 - (1 - \chi) \frac{h_{fg}}{C_p T} + \frac{V^2}{2C_p T} \quad (15)$$

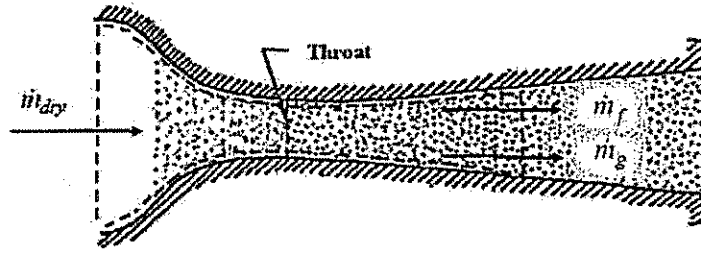


Figure 3: Schematic of mass flows into and out of the control volume (c.v.). The flow enters to the c.v. as dry with mass flow of \dot{m}_{dry} and leaves as two-phase with \dot{m}_f and \dot{m}_g . For the present study under steady-state conditions, $\dot{m}_{dry} = \dot{m}_f + \dot{m}_g$.

Using $C_p = \gamma R / (\gamma - 1)$, and defining:

$$M^2 \equiv \frac{V^2}{\gamma RT} \quad (16)$$

where M is the so called "the frozen Mach number", the Mach number obtained based on the gas-side (vapor) variables. Substituting Eqn. 16 into Eqn. 15:

$$\frac{T_{0,res.}}{T} = 1 - (1 - \chi) \frac{h_{fg}}{C_p T} + \frac{\gamma - 1}{2} M^2 \quad (17)$$

Equation 17 is an elegant equation that relates the local static temperature and Mach number in an arbitrary two-phase location. In the case of dry flows the quality χ is 1, and Eqn. 17 reduces Eqn. 9. Equation. 17, when compared to Eqn. 9 contains an extra term, $(1 - \chi)h_{fg}/C_p T \geq 0$. Therefore, for a given reservoir temperature, the local temperature T should be higher if condensation is allowed. That is due to the fact that the released latent heat of the condensate moves toward the vapor, and increases its temperature.

Equation 17 is what we planned to develop in the present section, a relation between the temperature and Mach number in two-phase region. However, we continue the present section and reword the term $(1 - \chi)h_{fg}/C_p T$ in a more friendly form. For the present isentropic expansion, the quality is obtained in terms of entropy as:

$$\chi = \frac{S_{0,res.} - S_f}{S_{fg}} \quad (18)$$

where both S_f and S_{fg} are functions of temperature only. With $S_{fg} = h_{fg}/T$, and $S_{fg} = S_g - S_f$. Therefore,

$$(1 - \chi) \frac{h_{fg}}{T} = S_g - S_{0,res.} \quad (19)$$

Defining

$$\zeta(T) \equiv \frac{S_g - S_{0,res.}}{C_p} \quad (20)$$

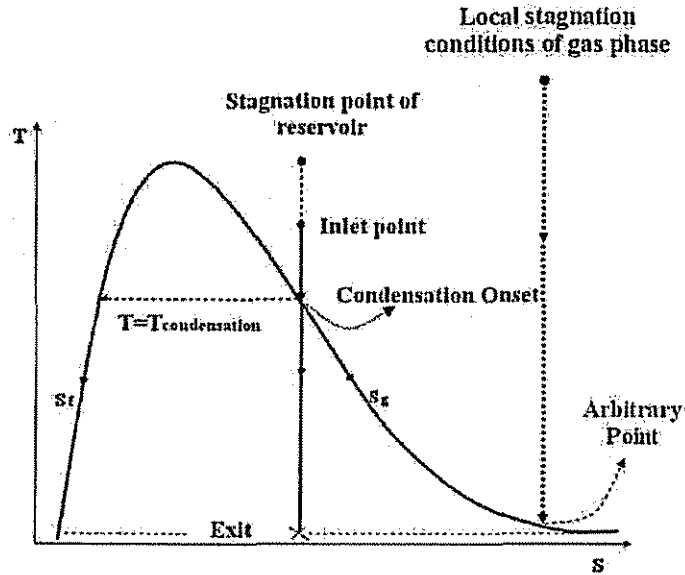


Figure 4: Defining a “local stagnation” condition for an “Arbitrary Point”. The “Arbitrary Point” represents the thermodynamic state of the vapor portion of the two-phase mixture. The “local stagnation” condition corresponds to the stagnation condition of the “Arbitrary Point”.

Equation 17 becomes:

$$\frac{T_{0,res.}}{T} = 1 - \zeta(T) + \frac{\gamma - 1}{2} M^2 \quad (21)$$

In Eqns. 20 and 21, $\zeta(T)$ is a non-dimensional function of only local temperature, which represents the entropy rise of the gas-side of the two-phase mixture. The source of this entropy rise is the reversible heat-release from the condensate towards the gas phase. It is noted that $\zeta(T) \geq 0$. The zero value corresponds to the process from “res.” to “c.o.”, while the > 0 represents the process beyond the “c.o.” under the saturation-dome. For the vapor portion of the two-phase mixture as a perfect gas, $\zeta(T)$ can alternatively be reworded into the following form:

$$\zeta(T) = \frac{1}{\gamma} \ln \left(\frac{P v_g^\gamma}{P_{0,res.} v_{0,res.}^\gamma} \right), \quad (22)$$

where the subscripts “g” and “0, res.” represent the states of the local gas phase (dry part of the two-phase mixture) and the reservoir, respectively, and $\gamma = 1.32$ for the vapor. As mentioned earlier, the process from reservoir to the “c.o.” point is isentropic. Therefore, $P_{c.o.} v_{c.o.}^\gamma / P_{0,res.} v_{0,res.}^\gamma = 1$, and $\zeta(T) = 0$ up to the “c.o.” point, where Eqn. 21 reduces to Eqn. 9.

3.2 Gas Phase Stagnation Conditions

In previous section it was shown that the stagnation conditions of a two-phase mixture cannot be determined using Eqn. 9, and an extra term of $\zeta(T)$ needs to be included for adjustments reasons (see Eqn. 21). However, a “local stagnation” condition for the vapor portion of the two-phase mixture (see Fig. 4) can be defined as:

$$\frac{T_{0,local}}{T} = 1 + \frac{\gamma - 1}{2} M^2 \quad (23)$$

$$\frac{P_{0,local}}{P} = \left(1 + \frac{\gamma - 1}{2} M^2\right)^{\gamma/\gamma-1} \quad (24)$$

where T and P are the local temperature and pressure of the two-phase mixture, and M is the Mach number of the vapor portion of the two-phase mixture:

$$M = V/\sqrt{\gamma RT} \quad (25)$$

known as "frozen Mach" number.

The stagnation conditions defined by Eqns. 23 and 24 correspond to the "arbitrary" exit section of the control volume shown in Fig. 3. The projection of the two-phase point along the saturated vapor curve is labelled as the "Arbitrary Point" and shown in Fig. 4. The stagnation conditions of the "Arbitrary Point" are noted as "Local stagnation conditions" in Fig. 4, which are obtained by Eqns. 23 and 24.

3.3 Conditions at Sonic Wet Throat

For wet flow arriving the sonic throat, the static temperature at the sonic throat is obtained using Eqn. 21, in which $M = M^* = 1$ at throat, where the superscript "*" refers to sonic state,

$$\frac{T_{0,res.}}{T^*} = 1 - \zeta(T^*) + \frac{\gamma - 1}{2} \quad (26)$$

Equation 26 is an equation of a single unknown T^* and can be solved for T^* . For the present wet-throat, the static pressure at the throat is set equal to the saturation pressure at T^* ,

$$P^* = P_{sat}(T^*) \quad (27)$$

where P_{sat} can be determined, for example, using Eqn. 39 in Appendix A. With T^* and P^* being known from Eqns. 26 and 27, the "local stagnation" conditions corresponding to the sonic wet throat are obtained by setting $M = 1$ in Eqns. 23 and 24,

$$\frac{T_{0,local}^*}{T^*} = \frac{\gamma + 1}{2} \quad (28)$$

$$\frac{P_{0,local}^*}{P^*} = \left(\frac{\gamma + 1}{2}\right)^{\gamma/\gamma-1} \quad (29)$$

Denoting the quality at the wet throat by χ^* , it can be obtained using Eqn. 18:

$$\chi^* = \frac{S_{0,res.} - S_f(T^*)}{S_{fg}(T^*)} \quad (30)$$

where S_{fg} and S_f are evaluated at the throat temperature, T^* . S_{fg} and S_f can be calculated using the relations provided in Appendix A.

3.4 Mass Flow through the Nozzle

For a two-phase (or wet) flow arriving the nozzle throat, Eqn. 11 is not suitable to predict the choked mass flow rate. Because the "local stagnation" conditions at the wet-throat are not equal to those of the reservoir, in this section, an equation is developed to predict the mass flow passing through a wet-throat nozzle. The accuracy of the developed equation has been assessed by our earlier numerical computation [7], and an excellent agreement is observed. Fig. 5 shows the comparisons.

In the present study the volume of the liquid is ignored in comparison to that of the gas. Therefore it can be shown that $\rho = \rho_g/\chi$, where ρ and ρ_g are the mixture and gas phase densities, respectively. If the vapor

portion of the two-phase mixture is taken as an ideal gas, ρ_g can therefore be obtained from $P_{sat}/(RT_{sat})$, and the mixture mass flow rate can be obtained from:

$$\dot{m} = \rho AV = \rho_g AV / \chi = \frac{\dot{m}_v}{\chi} \quad (31)$$

where A is the cross sectional area occupied by the two-phase mixture \approx cross sectional area occupied by the gas phase as the liquid volume is ignored, and V is the velocity of the mixture = velocity of each of the phases as the slip velocity between the phases is ignored. According to the classical thermodynamic theory, the vapor mass flow rate, $\dot{m}_v (= \rho_v A_v V_v)$, at any desired section along the nozzle can be obtained based on "local stagnation" conditions [6]:

$$\dot{m}_v = \frac{P_{0,local} A}{\sqrt{RT_{0,local}}} \sqrt{\gamma} \frac{M}{(1 + \frac{\gamma-1}{2} M^2)^{(\gamma+1)/2(\gamma-1)}} \quad (32)$$

The total (two-phase mixture) mass flow can, therefore, be obtained by:

$$\dot{m} = \frac{\dot{m}_v}{\chi} = \frac{P_{0,local} A}{\chi \sqrt{RT_{0,local}}} \sqrt{\gamma} \frac{M}{(1 + \frac{\gamma-1}{2} M^2)^{(\gamma+1)/2(\gamma-1)}} \quad (33)$$

The choked mass flow in a wet-throat nozzle is finally determined by setting $M = 1$ in Eqn. 33:

$$\dot{m}_{max(wet-throat)} = \frac{1}{\chi^*} \frac{P_{0,local}^* A^*}{\sqrt{R T_{0,local}^*}} \sqrt{\gamma \left(\frac{2}{\gamma+1}\right)^{\gamma+1/\gamma-1}}, \quad (34)$$

where χ^* , $P_{0,local}^*$ and $T_{0,local}^*$ are determined in Sec. 3.3.

Figure 5 compares the mass flow rates through a wet-throat nozzle obtained by (i) numerical computation of [7] and (ii) analytical solutions given by Eqn. 33. As shown in the figure, the flat profiles of these mass flow rates do agree very well with each other. This agreement implies that Eqn. 32 can correctly predict the local value of \dot{m}_v , obtained based on "local stagnation" conditions. It is noted that the decline in \dot{m}_v , in Fig. 5, is due to condensation. The condensate profile of \dot{m}_f (not shown in Fig. 5) can be obtained from $\dot{m}_f = \dot{m} - \dot{m}_v$. It is also noted that the value of the mass flow rate reflected by the flat profile in Fig. 5 represents the choked mass flow through the nozzle.

3.5 Relating A/A^* to Thermodynamic Properties

Combining Eqns. 33 and 34, a relationship for A/A^* can be obtained, where A is an arbitrary section along the nozzle and A^* is the cross sectional area of the sonic throat,

$$\frac{A}{A^*} = \left(\frac{P_{0,local}^*}{P_{0,local}}\right) \left(\frac{\chi}{\chi^*}\right) \left(\frac{T_{0,local}}{T_{0,local}^*}\right)^{\frac{1}{2}} \frac{1}{\left(\frac{\gamma+1}{2}\right)^{(\gamma+1)/2(\gamma-1)}} \frac{(1 + \frac{\gamma-1}{2} M^2)^{(\gamma+1)/2(\gamma-1)}}{M} \quad (35)$$

In general both A and A^* can be wet, and Eqn. 35 applies to both dry and wet cases. For dry flow through the sonic throat, $\chi^* = 1$, $T_{0,local} = T_{0,local}^* = T_{0,res.}$ and $P_{0,local} = P_{0,local}^* = P_{0,res.}$. In this case, Eqn. 35 is simplified to the classical equation for A/A^* in gas dynamics. For wet flows, the "local stagnation" conditions at the sonic throat are obtained using the relations provided in Sec. 3.3.

4 SUMMARY OF THE STEPS TO OBTAIN THE ANALYTICAL SOLUTION

The steps to obtain the analytical solution are summarized in this section. The flow-chart shown in Fig. 6, gives a step by step approach to obtain and fix the thermodynamic states at any arbitrary and desired location along the nozzle. As shown in Fig. 6, the flow-chart starts with known pressure and temperature of upstream reservoir for a given nozzle. The following steps explain the solution procedure:

Step 1 Obtain $S_{0,res.}$ using $T_{0,res.}$ and $P_{0,res.}$ of the reservoir from Eqn. 6.

Step 2 Solve Eqn. 8 to obtain $T_{c.o.}$. It is noted that $P_{c.o.}$ is the saturation pressure at $T_{c.o.}$, and can be obtained from Eqn. 39.

Step 3 (With $T_{c.o.}$ and $T_{0,res.}$ being known at this stage), obtain Mach number at "c.o." point using Eqn. 10.

Step 4 Determine if the nozzle throat is wet or dry. If $M_{c.o.} > 1$, then the "c.o." point is downstream of the throat and the throat is dry, see **Step (4-a)**. Otherwise $M_{c.o.} < 1$ and the throat is wet, as stated in **Step (4-b)**.

Step (4-a) The throat is dry, then the stagnation conditions at the throat are equal to those of the reservoir.

Step (4-b) The throat is wet, so the static temperature at the sonic wet throat, T^* , is obtained by solving Eqn. 26, and P^* is the saturation pressure at T^* , which is determined from Eqn. 27.

Step 5 Obtain the "local stagnation" conditions corresponding to the sonic wet throat, Eqns. 28 and 29.

At this stage the location of the "c.o." and the status of the nozzle throat (whether it is dry or wet) are known. In the following steps we start from the reservoir again and march along an expansion line until we meet the "c.o." point and the throat, and proceed further toward the nozzle exit.

Step 6 Select any value of T less than $T_{0,res.}$ and march along an expansion line from the reservoir toward the nozzle exit.

Step 7 Determine if the flow at the selected T is wet or dry. If $T > T_{c.o.}$ the flow is dry, see **Step (7-a)**. Otherwise it is wet, as stated in **Step (7-b)**.

Step (7-a) The flow is dry, then the "local stagnation" conditions are equal to those of the reservoir (i.e. $T_{0,local} = T_{0,res.}$ and $P_{0,local} = P_{0,res.}$), and the local Mach number is obtained from Eqn. 23.

Step (7-b) The flow is wet, then:

$$P = P_{sat}(T). \quad (36)$$

Using the definition of $\zeta(T)$, given by Eqn. 20, and the formula for $\chi(T)$, provided by Eqn. 18, we can write:

$$\zeta(T) = -\ln \frac{T_{0,res.}}{T} + \left(\frac{\gamma-1}{\gamma}\right) \ln \frac{P_{0,res.}}{P} \quad (37)$$

and

$$\chi(T) = 1 + \frac{(S_{0,res.} - C_p \ln T + R \ln P)}{h_{fg}/T} \quad (38)$$

Step 8 (With T being known), use Eqn. 21 to obtain the local Mach number at the present wet state.

Step 9 Determine the “local stagnation” values of $P_{0,local}$ and $T_{0,local}$ using Eqns. 23 and 24.

Step 10 Obtain the mass flows \dot{m}_v , and \dot{m} along the nozzle. The mass flow of the vapor portion of the two-phase mixture (\dot{m}_v) is determined using Eqn. 32. With that being known, the total mass flow is obtained using $\dot{m} = \dot{m}_v/\chi$. It is noted that $\chi = 1$ for dry regions, and $\dot{m} = \dot{m}_v$.

Step 11 Obtain the area ratio using Eqn. 35 throughout the nozzle.

5 COMPARISONS BETWEEN THE RESULTS

The developed analytical solutions are supported by experimental and numerical evidences. The computed pressure distributions along the nozzle axis are compared with those from experiments of [8] using nozzles (A) and (D). Figure 7 depicts the geometry of these nozzles.

Nozzle (A) has the highest expansion rate of these series of nozzles (i.e. the largest exit to throat area ratio) and nozzle (D) has the lowest expansion rate. The flow conditions are: $P_{0,res.} = 25$ kPa taken constant for all the nozzles geometries, $T_{0,res.A} = 354.6$ K, and $T_{0,res.D} = 361.8$ K. The outflow conditions for all cases are supersonic.

As shown in the figures (Figs. 8 to 11), the agreement between the numerical and analytical solutions are excellent, in fact they totally overlap for the most ranges. Their agreement with the experiment are quite good too, with differences between them owing to different choked mass flows through the nozzles which we explain briefly as follows, and complete details are given in [7]. Rapid expansion through the nozzles forces the flow to experience non-equilibrium conditions in real (experimental) case. Therefore condensation in the experiment does not begin until a significant amount of supercooling is achieved. This delays the moisture generation in the experiment, and it can be shown that flow is still dry in the nozzle throat if non-equilibrium model is used (see [9]).

6 CONCLUDING REMARKS

An analytical solution for the isentropic expansion of condensing two-phase steam flow is developed. The solution is validated with both numerical and experimental values. The highlights of the present solutions are given below:

- The developed formulae are given in a form similar to those of the isentropic expansion of single phase ideal gases.
- The “local stagnation” conditions, based on the conditions of the vapor portion of the two-phase mixture, are defined. These conditions are different from those of the inflow reservoir.
- The vapor mass flow is determined based on the “local stagnation” conditions, Eqn. 32.
- The total mass of the two-phase mixture has been obtained using Eqn. 33 and compared with the numerical computation of [7] in Fig. 5. Excellent agreements between the results are achieved.
- The vapor portion of the two-phase mixture has been assumed to obey the ideal gas equation of state. However, it is possible to model the vapor as a real gas using a more sophisticated equation of state, [12].

- A shock wave can also be included within the two-phase region in the diverging portion of nozzle. This is planned to be done in the continuation of the present work.

References

- [1] Nag, P. "Power Plant Engineering", Tata MacGraw-Hill, 2001.
- [2] Petr, V. & Kolovrant'k, M. 1994 " Laboratory and field measurements of droplet nucleation in expansion steam ". 12th Int. Conf. on Properties of Water and Steam, Sept. 11-16. FL, ASME.
- [3] Stastny, M. & Sejna, M. 1994 "Condensation effects in transonic flow through turbine cascade". 12th Int. Conf. on Properties of Water and Steam, Sept. 11-16. FL, ASME.
- [4] White, A. J., Young, J. B. & Walters, P. T. 1996 " Experimental validation of condensing flow theory for a stationary cascade of steam turbine blade". Phi. Trans. R. Soc. Lond. A354, 59-88
- [5] Guha, A. 1998 "A unified theory for the interpretation of total pressure and temprature in the two-phase flows at subsonic and supersonic speeds" Proc. R. Soc. Lond. A 454, 671-695
- [6] Moran, M.J. and Shapiro, H.N., "Fundamentals of Engineering Thermodynamics," 4th Edition, John Wiley & Sons, 1998.
- [7] Kermani, M.J., Gerber, A.G., and Stockie, J.M., Thermodynamically based Moisture Prediction using Roe's Scheme, The 4th Conference of Iranian AeroSpace Society, Amir Kabir University of Technology, Tehran, Iran, January 27-29, 2003.
- [8] Moore, M.J., Walters, P.T., Crane, R.I. and Davidson, B.J., "Predicting the Fog Drop Size in Wet Steam Turbines," Inst. of Mechanical Engineers (UK), Wet Steam 4 Conference, University of Warwick, paper C37/73, 1973.
- [9] Kermani, M. J., and Gerber, A. G. (2003) A General Formula for the Evaluation of Thermodynamic and Aerodynamic Losses in Nucleating Steam Flow, International Journal of Heat and Mass Transfer 46 (2003) 3265 3278
- [10] Van Leer, B., Towards the Ultimate Conservation Difference Scheme, V, A Second Order Sequel to Godunov's Method, J. Comput. Phys., Vol. 32, pp. 110-136, 1979.
- [11] Hoffmann, K. A. and Chiang, S. T., "Computational Fluid Dynamics for Engineers", Vol. II, A Publication of Engineering Education Systems, Wichita, Kansas, USA, 1993.
- [12] M. J. Kermani, M. Zayernouri, and M. Saffar Avval, Development of a New Thermodynamic Chart for Isentropic Expansion of Condensing Steam Flow, The ISME Conference, June 2006, Isfahan, Iran.

Appendix

Saturated Pressure Value. The saturation pressure for steam is determined by a fifth order polynomial least square curve fit to the steam data taken from [6], given by:

$$p_{sat} = A_5(T - t_0)^5 + A_4(T - t_0)^4 + A_3(T - t_0)^3 + A_2(T - t_0)^2 + A_1(T - t_0) + A_0, \quad (39)$$

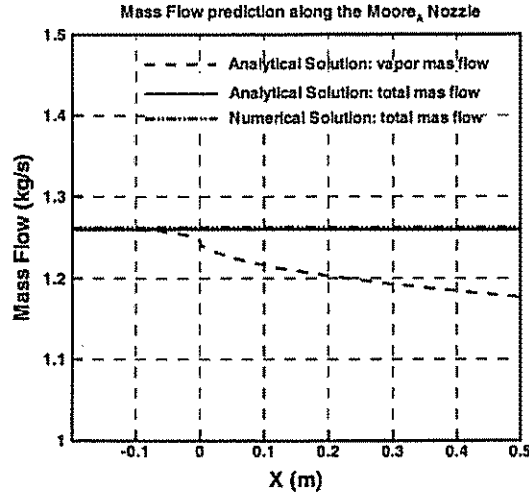


Figure 5: Comparison of numerical and analytical solutions for the mixture, $\dot{m}_f + \dot{m}_v$, mass flow through a wet-throat nozzle. \dot{m}_v is the mass flow rate of the vapor portion of the two-phase mixture, where its decline represents the condensation rate.

where p and T are in terms of Pa and K , $t_0 = 273.15 K$, accurately predicting saturated pressure in the range of $T = [293, 423] K$. The coefficients are

$$\begin{aligned}
 A_5 &= +1.777491E-6 \\
 A_4 &= +5.818105E-4 \\
 A_3 &= -8.508110E-3 \\
 A_2 &= +3.282639E+0 \\
 A_1 &= +1.313810E+0 \\
 A_0 &= +9.635917E+2
 \end{aligned} \tag{40}$$

Internal Energy. Internal energy is obtained by a parabolic curve fit to the steam data taken from [6], as

$$e_{fg} = E_2(T - t_0)^2 + E_1(T - t_0) + E_0, \tag{41}$$

where T is measured in K , e_{fg} is in J/kg ,

$$\begin{aligned}
 E_2 &= -1.964125E+0 \\
 E_1 &= -2.661665E+3 \\
 E_0 &= +2.372678E+6
 \end{aligned} \tag{42}$$

Therefore, $h_{fg} = e_{fg} + RT$, where $R = 461.3990 J/kg.K$ for vapor, as an ideal gas.

Entropy. The entropy of the mixture is determined from $s = s_f + \chi s_{fg}$, where $s_{fg} = h_{fg}/T$ and s_g is obtained from $s_g = C_p \ln T - R \ln p$, and $s_f = s_g - s_{fg}$.

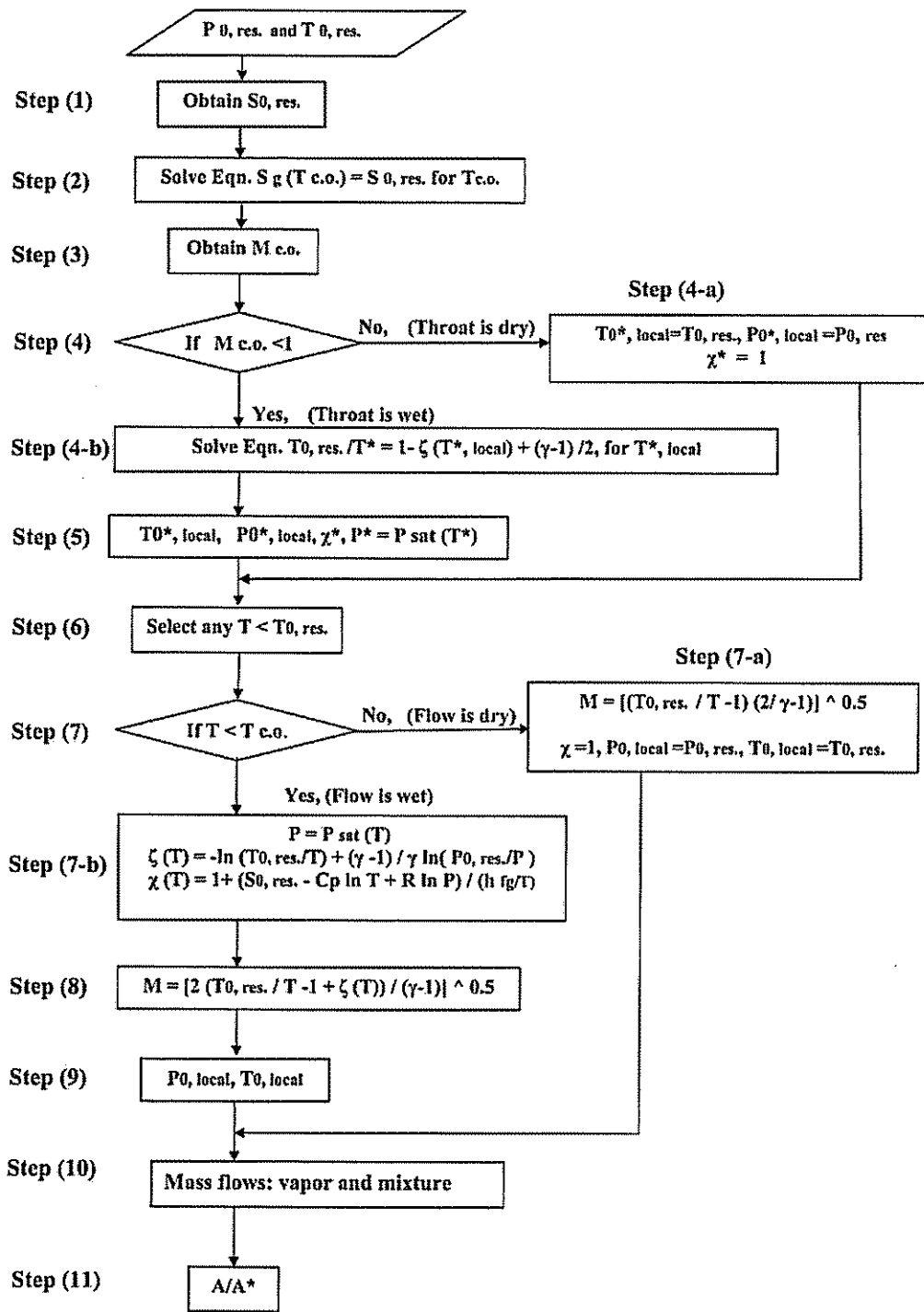


Figure 6: Algorithm of analytical solution.

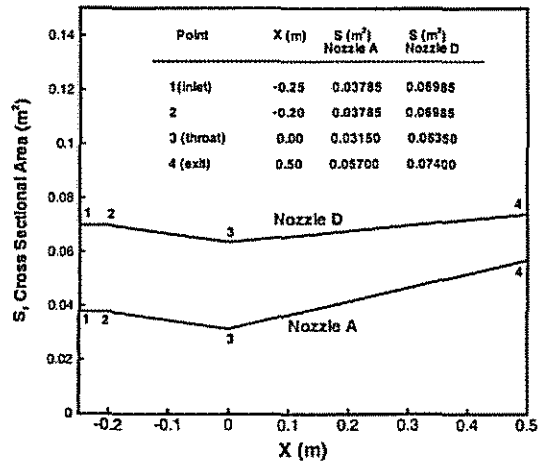


Figure 7: Geometry of the nozzle used in the present study.

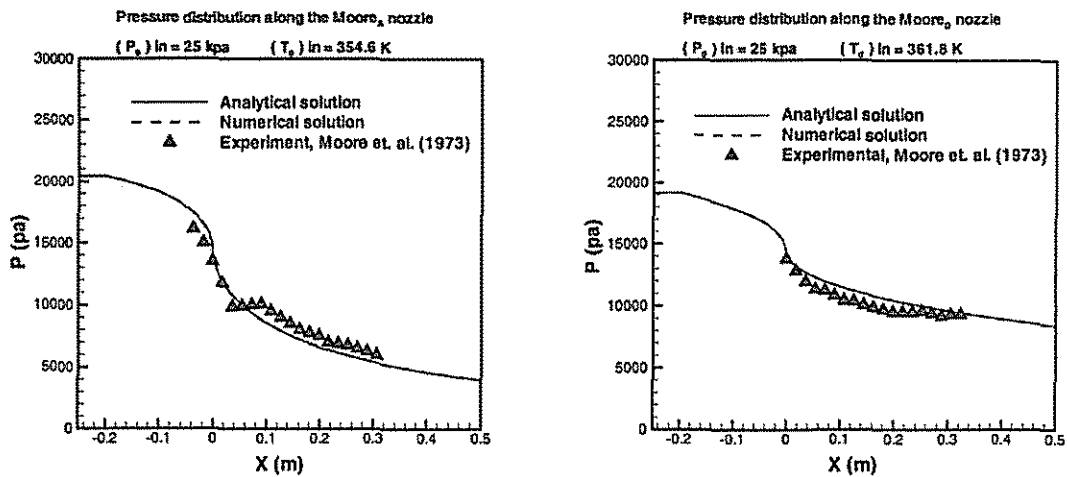


Figure 8: Comparison of pressure distribution along the nozzle centerline, Left: $Moore_A$ nozzle, Right: $Moore_D$ nozzle.

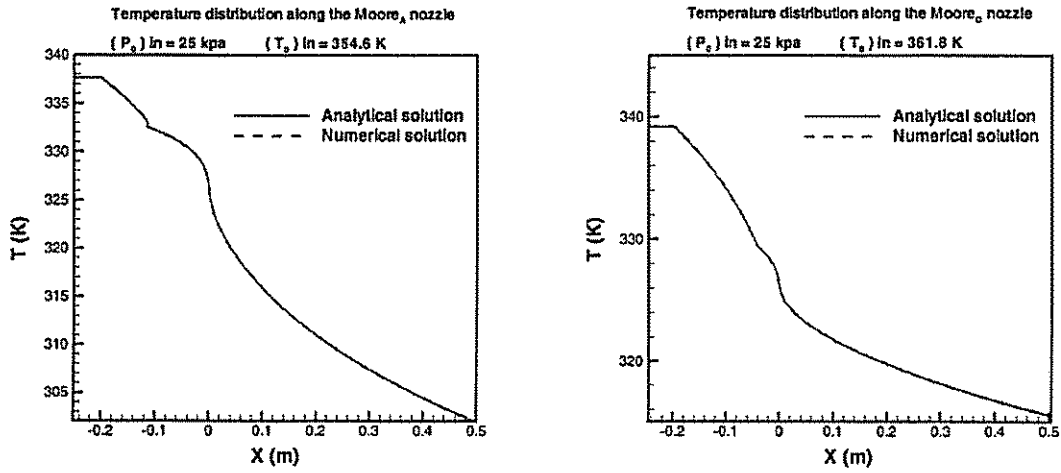


Figure 9: Comparison of temperature distribution along the nozzle centerline, Left: *Moore_A* nozzle, Right: *Moore_D* nozzle.

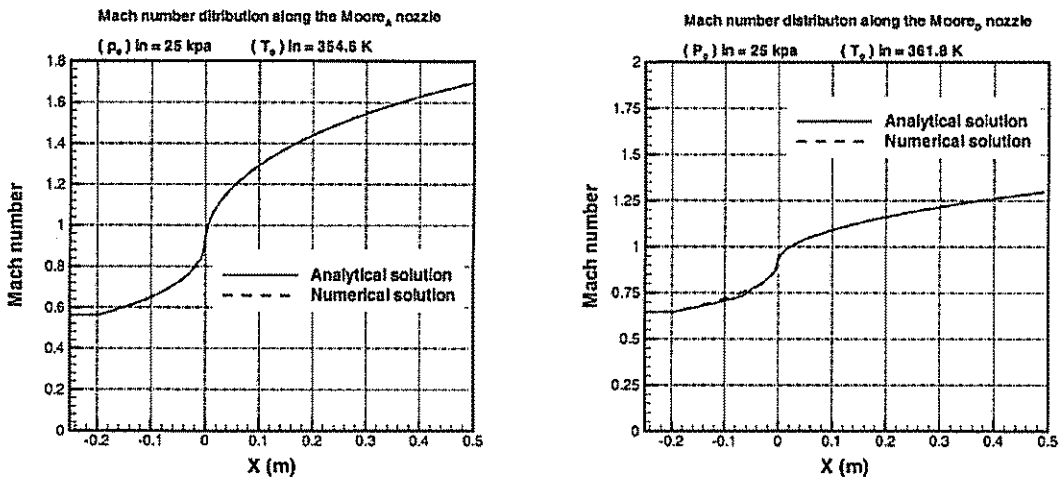


Figure 10: Comparison of Mach number distribution along the nozzle centerline, Left: *Moore_A* nozzle, Right: *Moore_D* nozzle.

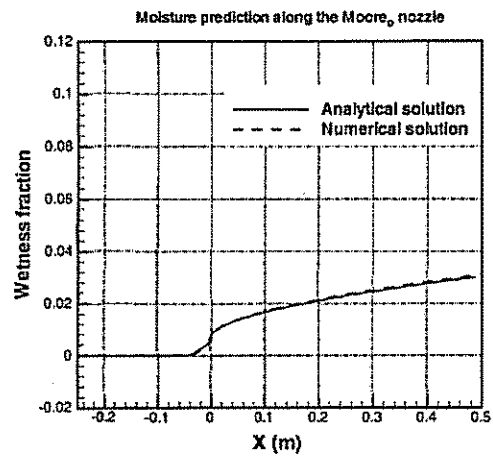
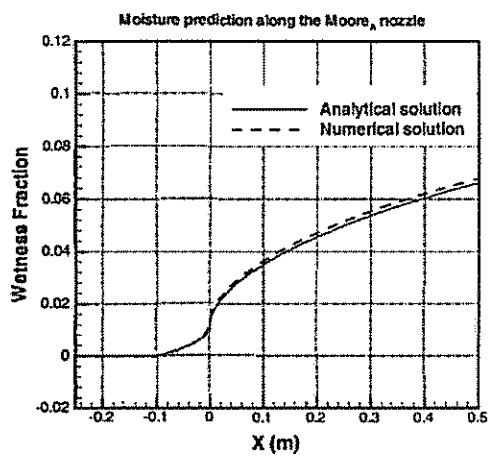


Figure 11: Comparison of moisture prediction distribution along the nozzle centerline, Left: *Moore_A* nozzle, Right: *Moore_D* nozzle.